

# Title Page Title: The role of DNA methylation in the accumulation of iridoid glycosides in *Rehmannia glutinosa*

**Tianyu Dong**

Henan Normal University

**Xiaoyan Wei**

Henan Normal University

**Qianting Qi**

Henan Normal University

**Peilei Chen**

Henan Normal University

**Yanqing Zhou**

Henan Normal University

**Yongkang Liu**

] Agricultural Research Institute of Wenxian County

**Cuihong Lu**

] Agricultural Research Institute of Wenxian County

**Hongying Duan** (✉ [Duanhy536@163.com](mailto:Duanhy536@163.com))

Henan Normal University

---

## Research Article

**Keywords:** epigenetic, DNA methylation, secondary metabolism, iridoid glycosides.

**Posted Date:** April 20th, 2021

**DOI:** <https://doi.org/10.21203/rs.3.rs-403607/v1>

**License:** © ⓘ This work is licensed under a Creative Commons Attribution 4.0 International License. [Read Full License](#)

---

# Abstract

**Background:** Epigenetic regulation plays a significant role in the accumulation of plant secondary metabolites. The terpenoids are the most abundant in the secondary metabolites of plants, iridoid glycosides belong to monoterpenoids which is one of the main medicinal components of *R.glutinosa*. At present, study on iridoid glycosides mainly focuses on its pharmacology, accumulation and distribution, while the mechanism of its biosynthesis and the relationship between DNA methylation and plant terpene biosynthesis are seldom reports.

**Results:** The research showed that the expression of *DXS*, *DXR*, *10HGO*, *G10H*, *GPPS* and accumulation of iridoid glycosides increased at first and then decreased with the maturity of *R.glutinosa*, and under different concentrations of 5-azaC, the expression of *DXS*, *DXR*, *10HGO*, *G10H*, *GPPS* and the accumulation of total iridoid glycosides were promoted, the promotion effect of low concentration (15 $\mu$ M-50 $\mu$ M) was more significant, the content of genomic DNA 5mC decreased significantly, the DNA methylation status of *R.glutinosa* genomes was also changed. DNA demethylation promoted gene expression and increased the accumulation of iridoid glycosides, but excessive demethylation inhibited gene expression and decreased the accumulation of iridoid glycosides.

**Conclusion:** The analysis of DNA methylation, gene expression, and accumulation of iridoid glycoside provides insights into accumulation of terpenoids in *R.glutinosa* and lays a foundation for future studies on the effects of epigenetics on the synthesis of secondary metabolites.

## Background

Plant secondary metabolism plays an important role in plant growth and development, environmental adaptation, resistance to diseases and insect pests [1]. According to their chemical structure, plant secondary metabolites can be mainly divided into terpenoids, phenols and nitrogen-containing compounds. Terpenes are widely distributed and varied, and they are the most common secondary metabolites in plants. All terpenes are synthesized from the isoprene unit isoprene diphosphate (IPP) and its isomer dimethylallyl diphosphate (DMAPP) [2]. Iridoids belong to monoterpenes and studies have shown that the biosynthetic precursors of plant ester terpenes (IPP and DMAPP) mainly come from the 2-C-methyl-D-erythritol-4-phosphoric acid (MEP) pathway [3–5].

The MEP pathway was originally identified in bacteria in the mid-1990s and later discovered in plants [6, 7], and can produce both IPP and DMAPP simultaneously from pyruvate and D-glyceraldehyde 3-phosphate (GAP) via seven consecutive steps [8]. The MEP pathway provides the reaction precursors IPP and DMAPP, in the catalysis of geranyl pyrophosphate synthase(GPPS), the form of geranyl diphosphate is produced, and in the presence of geraniol synthase(GES), the form of geraniol is produced, and then in the phloem epidermal cells (IPAP), under the catalysis of various functional enzymes, such as 10-geraniol hydroxylase(G10H), 10-hydroxygeranioloxidoreductase(10-HGO), iridoid synthase(IS), 7-deoxyloganetic acid synthase(7-DLS), 7-deoxyloganetic acid glucosyltransferase(7-DLGT) and 7-deoxyloganicacid hydroxylase(7-DLH),oxidation, reduction, glycosylation and methylation reactions were carried out to form loganicacid, loganicacid generates secologanin under the catalysis of loganic acid methyltransferase (LAMT) and secologanin synthase (SLS) which has the skeleton structure of iridoid glycosides [9–11]. In the whole process of iridoid glycoside synthesis, the study of related enzymes is mainly focused on a series of key enzymes in MVA and MEP pathway and

terpene synthase which catalyze the formation of iridoid glycoside skeleton, 1-deoxyxylulose-5-phosphate synthetase(DXS) catalyzes pyruvate and glycerol-3-phosphate to produce 1-deoxyxylulose-5-phosphate (DXP), which is the first rate-limiting enzyme in this pathway [12], *DXS* silencing leads to albinism in *Arabidopsis thaliana*[13], Overexpression of *DXS* leads to the increase of carotenoid and vitamin E content [14]. 1-deoxy-D-xylulose-5-phosphate reductase (DXR) catalyzes the synthesis of terpenoid skeleton, catalytic rearrangement of 1-deoxy-D-xylulose-5-phosphoric acid (DXP) to form MEP[15, 16], inhibition of *DXR* expression, the content of artemisinin decreased significantly in *Artemisia annua L* [17]. GPP, the precursor of monoterpenes synthesized by IPP and DMPP catalyzed by GPPS, is the first step in the synthesis of monoterpenes [18, 19], which is responsible for the formation of GPP towards most monoterpenes and diterpenes in plastids [20, 21]. G10H is a key enzyme in the synthesis of monoterpenes, which can catalyze the hydroxylation of geraniol to 10-hydroxygeraniol [22, 23], *G10H* overexpression significantly increased the accumulation of strictosidine, vindoline and catharanthine [24]. 10HGO is an important component in the biosynthesis pathway of iridoterpene glycosides, and also is a NADPH-dependent cytochrome P450 monoterpene oxidase which can catalyze the oxidation of 10-hydroxygeraniol to 10-hydroxy geraniol [25, 26].

DNA methylation, in combination with histone modifications and non-histone proteins, defines chromatin structure and accessibility. DNA methylation therefore helps to regulate gene expression, transposon silencing, chromosome interactions and trait inheritance [27]. DNA methylation affects the accumulation of plant secondary metabolites and the expression of related enzyme genes in the secondary metabolism pathway. Transgenic tobacco plants overexpressing *Arabidopsis thaliana* demethylase gene *ROS1* significantly increased the expression of flavonoid metabolism and antioxidant pathway genes, thus improving the salt tolerance of transgenic tobacco [28]. In transgenic *hybrid poplars* overexpressing chestnut demethylase gene, the expression of flavonoid biosynthesis was promoted, the accumulation of flavonoids in apical meristem and the maturation of scale bud and apical bud were also promoted [29]. After NaCl stress, 12 genes were significantly enriched by hypermethylation in the leaves of tetraploid watermelon seedlings, involving the biosynthesis of cork grease, wax and monoterpenes and transcriptome results showed that diploid watermelon roots were regulated by DNA demethylation and 8 genes in linoleic acid metabolism pathway were up-regulated [30]. Methylation inhibitors affect the expression of related genes in the metabolic pathway, which in turn affects the accumulation of secondary metabolites. 5azaC can activate energy metabolism pathway, pentose phosphate pathway, fatty acid metabolism pathway and other biological pathways and these pathways can provide material and energy basis for paclitaxel synthesis, such as NADPH, energy, acetyl-CoA, Glyceraldehyde triphosphate, at the same time, 5azaC stimulates the expression of key enzyme genes in paclitaxel synthesis pathway, and paclitaxel content increases continuously with the decrease of methylation level [31, 32]. The genes in differential methylation region between the roots of *Salvia miltiorrhiza* at two stages were enriched in the diterpene biosynthesis pathway, 5azaC treatment of *Salvia miltiorrhiza* hairy roots growing for two months could significantly increase the biosynthesis of tanshinones, indicating that DNA methylation was involved in the biosynthesis of tanshinones [33, 34]. The expression of key enzyme genes (*hmgr*, *sqs*, *se* and *ls*) in *Ganoderma lucidum* biosynthesis was increased after 5azaC treatment, and the accumulation of ganoderic acid in *Ganoderma lucidum* was also increased, even 5azaC treatment decreased the level of genomic DNA methylation, it did not change the methylation level of *sqs*, *ls* and *se* gene promoter region [35]. NO increased the level of DNA methylation in cultured *Robinia pseudoacacia* cells, and the change trend was dynamically related to isoflavone synthesis and 5azaC blocked isoflavone synthesis induced by nitric oxide [36]. The contents of polysaccharides and alkaloids in *Dendrobium* increased significantly under 5azaC treatment[37]. To sum up, DNA methylation is

necessary to maintain normal plant growth, and plays an indispensable regulatory role in plant gene expression, cell differentiation, phylogeny and accumulation of secondary metabolites.

Although some progress has been made in the accumulation of secondary metabolites by DNA methylation in plants, it is still mainly focused on the relationship between total DNA methylation level and the content of plant secondary metabolites, and lack of molecular mechanism of DNA methylation in the accumulation of secondary metabolites, especially in *R. glutinosa*, there are few studies on the relationship between DNA methylation and iridoid glycoside accumulation, and the effect of DNA methylation on the expression of key enzyme genes in iridoid glycoside synthesis pathway. In view of the close relationship between plant secondary metabolism and epigenetics, the purpose of this study is to reveal the changes of gene expression and secondary metabolites at the epigenetic level and hope to explore the mechanism of the formation of plant secondary metabolites.

## Materials And Methods

### Plant materials

In this study, *R. glutinosa* cultivar (85 – 5, Jinjiu) was chosen, and its root tubers were kindly provided by Agricultural Research Institute of Wenxian County, Henan, China. Primers were synthesized by Yingjieji Trade Co., Ltd., (Shanghai, China) and their sequences are listed in **Table S1**.

In addition, LYK and LCH, agronomists of Agricultural Research Institute of Wenxian County, have formally identified the experimental materials *Rehmannia glutinosa* 85 – 5 and Jinjiu, and these experimental materials have not been deposited in a publicly available herbarium.

### Treatment and Cultivation of *R. glutinosa*

After sterilized for 10 min by 0.1% HgCl<sub>2</sub>, root tubers of *R. glutinosa* were washed for 3–5 min with sterile water, and were wrapped with gauze, then were respectively treated for 7d (3 times/d) with 0, 15, 30, 50, 100 or 250 μM 5-azaC. Subsequently, root tubers treated with 5-azaC were grown in test field, College of Life Science, Henan Normal University, Xinxiang City, Henan Province, China. In addition, 100 sterilized roots of *R. glutinosa* were treated with 5-azaC in each group, and there were three replicates per group.

Stage I: seedling root is not fleshy

Stage II: plant root is fleshy and cylindrical

Stage III: plant root appears preliminary expansion

Stage IV: plant root appears middle expansion

Stage V: plant root appears late expansion

Tuberous root and leaf of *R. glutinosa* at each growth stage were frozen in liquid nitrogen and stored at -80°C.

### Genomic DNA extraction of *R. glutinosa*

Genomic DNA was extracted from root and leaf of *R. glutinosa* by CTAB method with modifications [38]. About 4 g tuberous root or leaf was put into the pre-cooled mortar and ground into the powder, then immediately transferred to 50mL centrifuge tube. In the centrifuge tube, 5mL/g CTAB solution containing two-thousandths of  $\beta$ -mercaptoethanol was added, and put in water bath at 65°C for 2 h accompanied by upside down mixing 1 times/20 min, centrifuged for 10 min at 12000rpm. Afterwards, the supernatant was transferred, extracted by phenol:chloroform:isoamyl alcohol (25:24:1) and centrifuged for 10 min at 12000 rpm. The above process was repeated once, and then the supernatant with isopropyl alcohol was placed for more than 1h and separated by 12000rpm centrifugation for 15 min. Precipitated DNA was washed twice with 70% ethanol, and dissolved in double-distilled water after air dried for at least 5 min, then 1% RNase was added to DNA solution; put at 37°C for 30min and extracted with phenol:chloroform:isoamyl alcohol (25:24:1). After further extraction, DNA solution was precipitated by adding 1/3 volume of 3 M NaAc and 2.5 volumes of absolute ethanol, and centrifuged at 12000 rpm for 10 min, then precipitated DNA was washed twice with 70% ethanol and centrifuged at 12000 rpm for 5 min. Subsequently, dried DNA was dissolved in double-distilled water and was stored at -20°C to analyze genomic DNA methylation.

In addition, the integrity of genomic DNA was detected by 0.8% agarose gel electrophoresis, and the yield and purity of genomic DNA were respectively determined by spectrophotometry at 260nm.

#### **Total RNA extraction and first-strand cDNA preparation**

Total RNA was extracted from root and leaf samples using an RNA kit (Bio-Connect, Huissen, Netherlands). RNA concentration and purity were estimated spectro-photometrically based on absorbance at 260 and 280 nm. First-strand cDNA was synthesized from 1  $\mu$ g total RNA, which was reversely transcribed using M-MLV reverse transcriptase with oligo (dT) 15 as a primer in a 10 $\mu$ L reaction volume (Takara, Japan).

#### **Cloning of *DXS*, *DXR*, *10HGO*, *G10H* and *GPPS***

The sequences of *DXS*, *DXR*, *10HGO*, *G10H* and *GPPS* genes of *R. glutinosa* were obtained by electronic cloning. The partial sequences of the genes obtained by transcriptome sequencing were used as probes, and the online database of *R. glutinosa* SRA (SequenceReadArchive) sequence in NCBI was searched by Blastn tool. The SRA sequence of *R. glutinosa* which has the same homology with the probe sequence was obtained, which was compared, spliced and extended by DNAMAN7.0, and then the extended overlap group (Contig) was used as the probe, then Blastn retrieval is carried out through the SRA database until there is no new SRA sequence to be spliced and the overlap group can not be extended.

According to the sequence obtained by electronic cloning technology, the corresponding primers were designed and PCR amplification was carried out with *R. glutinosa* cDNA as template. The PCR amplification system was as follows: template 2.0 $\mu$ L, Primer-F(10 $\mu$ M) 1.0 $\mu$ L, Primer-R(10 $\mu$ M) 1.0 $\mu$ L, 2xTaqMix 10 $\mu$ L, sterilized ddH<sub>2</sub>O 6.0 $\mu$ L. PCR amplification program is: 95°C, 3min; 95°C 30 s, annealing 30s (*DXS* 52°C, *DXR* 50°C, *10HGO* 50°C, *G10H* 54°C, *GPPS* 55°C), 72°C 2min, a total of 34 cycles, 72°C extension 10min. The PCR product was cut and recovered, and then the target fragment was connected with the T vector, and the ligated product was transformed into *Escherichia coli*. The PCR product was detected by agarose gel electrophoresis, and the bacterial solution of the same size as the target band was sent to the company for sequencing. The bacterial solution with correct sequencing was mixed with 50% glycerol and stored at -20°C.

#### **Quantitative Real-time PCR**

*TIP41* was used as internal reference gene, the primers of *TIP41*, *DXR*, *DXS*, *10HGO*, *G10H* and *GPPS* are q*TIP41*-F, q*TIP41*-R, q*DXSF*, q*DXSR*, q*DXRF*, q*DXR*-R, q*10HGO*-F, q*10HGO*-R, q*G10HF*, q*G10HR*, q*GPPSF*, q*GPPSR*, respectively. According to the AceQ Qpcr SYBR Green MasterMix kit (Vazyme, Nanjing, China) instructions, the configuration of the reaction system is carried out on the ice, and the whole operation avoids light and avoids the failure of the reagent. The fluorescence quantitative PCR reaction was carried out on the LightCycler96 fluorescence quantitative PCR instrument. The PCR amplification system is as follows: template 2.0μL, Primer-F (10μM) 0.5μL, Primer-R (10μM) 0.5μL, SYBR Green Master Mix 10μL, sterilized ddH<sub>2</sub>O 20.0μL. The PCR amplification program is: 95°C, 5min; 95°C 10 s, 60°C 30 s, a total of 40 cycles; 95°C 15 s, 60°C 60 s, 95°C 15 s.

Excel was used for statistics and calculation, and the expression of the target gene in the sample was calculated by  $2^{-\Delta\Delta C_t}$  method. In the later experiment, GraphPad Prism 5.0 software was used, and the data were analyzed by least significant difference (LSD) multiple comparison.

### **Determination of iridoid glycosides in *R. glutinosa***

The fresh roots and leaves of *R. glutinosa* (cut into thin slices) were put into the oven, dried at 50°C for 48 hours, and the powder was pressed by a grinder. Accurately weigh 1g of *R. glutinosa* powder into a 100mL plug conical bottle, add 10 mL of 70% ethanol solution, ultrasonic extraction for 45 minutes, supplement the weight, filter the filtrate (qualitative filter paper and inorganic filter head double filtration). Put the filtrate into the 50mL volumetric flask and shake, accurately measure 2.5mL in the 50mL volumetric flask and fix the volume. Accurate weighing of catalpol reference substance 5.76mg was placed in a 25mL volumetric bottle and 70% ethanol constant volume (0.23mg/mL) control solution was added. Catalpol control solution 1.5ml, 2.0ml, 2.5ml, 3.0ml, 3.5ml and 4.0ml were respectively taken and placed in a 10mL volumetric flask, and then 70% ethanol was added for constant volume. Take the control solution, test solution and 70% ethanol (blank control) 1mL into the 10mL plug test tube, add 1mol LHCL 2ml, 90°C water bath 15min, room temperature 15min cool, add dinitrophenylhydrazine ethanol test solution 0.5ml, 90°C water bath 25min, room temperature 15min cool, add 1molL NaOH 70% ethanol solution 30ml, place at room temperature for 1 hour. With 70% ethanol as a blank, the absorbance was determined at 463nm. The data were sorted out by Excel and SPSS software, and multiple comparisons were made by Duncan method in the analysis of variance.

### **HPLC Detection of Genomic Methylation**

The content of 5-methyl cytosine (5mC) usually indicates the level of genomic DNA methylation. In this research, level of DNA methylation was detected by HPLC (high performance liquid chromatography) [38]. After genomic DNA of *R. glutinosa* was orderly hydrolyzed with DNase I, nuclease P1 and alkaline phosphatase, was centrifuged at 12000rpm for 5min, then the supernatant was transferred and was filtered with 0.45μM organic microfiltration membrane, subsequently was detected by HPLC. These chromatography conditions performed in this study were as follows: the mobile phase was composed of 50mM KH<sub>2</sub>PO<sub>4</sub> and 8% methanol (92: 8), the flow velocity was 0.5ml/min, the column temperature was 30°C, the sensitivity was 0.1, the injection volume was 20μl, the analytical column was Agilent C18 Zorbax XDB column (4.6×150mm, 5μm particle size), and the detection wavelength was 285nm.

The standard substance of 0.0044g C and 0.0065g 5mC was separately dissolved with 10ml ultra pure water to 40nM/100μL (mother liquor), and the mother liquor was diluted to 0.02nM/100μl, 0.05nM/100μl,

0.1nM/100µl, 0.5nM/100µl, 1nM/100µl, then each concentration of standard substance (20µl) was detected. As shown in HPLC chromatogram, the standard substance of C and 5mC both had a good linear relationship in the range of 0.02-1.0nM/100µl, and the linear equation of C or 5mC as follows:  $y = 2172.7x - 18.537$  ( $R^2 = 0.9993$ ),  $y = 2276x - 7.9806$  ( $R^2 = 0.9997$ ), in which x or y represented concentration and peak area of standard substance respectively. According to the above linear equation of standard substance C and 5mC, the concentration of C and 5mC could be respectively calculated, then the content of 5mC was obtained according to the following formula:  $5mC = [5mC / (5mC + C)] \times 100$ . In addition, precision, repeatability and stability of HPLC were tested to guarantee the reliability of experiment data, and the detection of C and 5mC in genomic DNA was repeated three times.

### **Methylation-Sensitive Amplified Polymorphism (MSAP) Amplification**

The MSAP experiment was performed with modifications according to the method of Pieter et.al [39]. Under the condition of without changing methylation status, HpaII and MspI have different sensitivity to DNA methylation. HpaII is not sensitive to full methylation (double-stranded-methylation) and could cleave hemi-methylation (single-stranded-methylation), MspI is sensitive to the internal cytosine (CmCGG sequence) and not to the external cytosine (mCCGG sequence) in full methylation. Thus, HpaII and MspI were selected to produce different cleavage fragments which can reveal status and extent of genomic DNA methylation. Genomic DNA of *R. glutinosa* was digested with endonuclease EcoRI/MspI, EcoRI/HpaII, in turn, then was ligated with EcoRI adapter and MspI-HpaII adapter by T4 DNA ligase at 16°C for 15 h, subsequently Enzyme-Ligation product was stored at -20°C.

After the pre-amplification system of MSAP was established, Enzyme-ligation product was diluted 10-fold and amplified as a pre-amplification template. The reaction system of MSAP pre-amplification was 50µL and consisted of 2.5µM EcoRI pre-amplification primer, 2.5µM MspI-HpaII pre-amplification primer, 25µL 2×Taq Mix, 0.5µL Enzyme-Ligation product, and cycling conditions of PCR pre-amplification were: 72°C 1min, 94°C 45s, 65°C 30s, 72°C 1min; 94°C 30s, 64.3°C annealing for 30s, 72°C 1min, 12 cycles, each cycle annealing temperature drop low 0.7 °C; 94°C 30s, 55.9°C 30s, 72°C 1min, 20cycles; 72°C 30min. After amplification, results of pre-amplification were detected by 1% agarose gel electrophoresis, the pre-amplification product was diluted 10-fold and amplified as template in MSAP selective amplification. The reaction system of MSAP selective amplification was 20µL and composed of 5µM EcoRI selective amplification primer, 5µM MspI/HpaII selective amplification primer, 10µL 2×Taq Mix and 0.5µL pre-amplification product. Furthermore, the reaction condition of MSAP selective amplification was the same as pre-amplification except without Pre-PCR\_1, subsequently amplification products were detected by 6.0% polyacrylamide gel electrophoresis.

### **MSAP Data Analysis**

In this research, DNA methylation level was quantified by MSAP binary data, the presence or absence of one band was respectively scored as "1" and "0", only clear and reproducible bands were scored after silver staining. For MSAP analysis, bands were scored on the basis of presence or absence in EcoRI/HpaII (H) and EcoRI/MspI (M), and the banding patterns of MSAP amplification could be divided into three classes: the presence of band in H and M was considered no methylation (class I), the presence of band only in H was considered DNA hemi-methylation (class II), and the presence of band only in M was considered DNA full-methylation (class III). In addition, DNA methylation level was calculated with the following formula:  $\text{DNA methylation level (\%)} = (\text{bands of class II} + \text{bands of class III}) / (\text{bands of class I} + \text{bands of class II} + \text{bands of class III}) \times 100$ , DNA hemi-

methylation level (%) = bands of class II/(bands of class I + bands of class II + bands of class III) ×100, DNA full-methylation level (%) = bands of class III/(bands of class I + bands of class II + bands of class III) ×100.

Compared with the control, DNA methylation patterns of *R. glutinosa* treated with 5-azaC were classified into methylation polymorphism and methylation monomorphism. DNA methylation monomorphism was regarded Type A, DNA methylation polymorphisms included type B (DNA methylation) and type C (DNA demethylation).

### Statistical Analysis

In this research, gene expression, iridoid glycosides content, 5mC content and methylation level of *R. glutinosa* were tested for significance level, by using analysis of variance and multiple comparisons of Duncan's multiple range. Gene expression, content of iridoid glycosides, content of 5mC and level of DNA methylation were calculated and analyzed by Excel and DPS7.5, and all histograms were drawn by Graphpad Primer 5.0.

## Results

### Cloning and bioinformatics analysis of *DXS*, *DXR*, *10HGO*, *G10H* and *GPPS*

We cloned *DXS*, *DXR*, *10HGO*, *G10H* and *GPPS* genes from *R. glutinosa* and registered them in GenBank, *DXS* (MG764508), *DXR* (MG764509), *10HGO* (MH102394), *G10H* (MK559439), *GPPS* (MG770219), their cDNA length is 2380bp, 1751 bp, 1192 bp, 2020 bp, 1314 bp, CDS length is 2154 bp, 1479 bp, 1065 bp, 1473 bp, 1272 bp, respectively. *DXS* has 8 exons and 7 introns, and none of the other genes have introns (Table 1, Fig. S1). The analysis of protein physical and chemical properties showed that the molecular weight (MW) of *DXS*, *DXR*, *10HGO*, *G10H* and *GPPS* proteins were 77.12KD, 53.48 KD, 38.44 KD, 55.21 KD, 46.34 KD, PI were 6.80, 5.79, 6.21, 8.81, 6.04 respectively, and *DXR* and *10HGO* were hydrophobic. The secondary structure prediction shows that the  $\alpha$  helix ratio is 24.01–57.82%, and the  $\beta$ -folding ratio is 3.55–8.94%. The prediction of subcellular localization showed that *10HGO* was located in the cytoplasm and the others were located in the chloroplast (Table 2).

Table 1  
Sequence information of *DXS*, *DXR*, *10HGO*, *G10H*, *GPPS* synthase genes in *R. glutinosa*

Gene Name	Accession Number	cDNA Length (bp)	CDS Length (bp)	No. of Extron
<i>DXS</i>	MG764508	2380	2154	8
<i>DXR</i>	MG764509	1751	1479	1
<i>10HGO</i>	MH102394	1192	1065	1
<i>G10H</i>	MK559439	2020	1473	1
<i>GPPS</i>	MG770219	1314	1272	1

Table 2  
The analysis of *DXS/DXR/10HGO/G10H/GPPS* proteins in *R. glutinosa*

Protein Name	No.of AA	Physico-chemical Property			Secondary Structure				Subcellular location
		MW (kD)	PI	hydrophilicity	Alpha helix (%)	Extended strand (%)	Beta turn (%)	Random coil (%)	
DXS	717	77.12	6.80	hydrophilicity	38.77	15.62	6.42	39.19	Chloroplast
DXR	492	53.48	5.79	hydrophobicity	34.35	19.92	8.94	36.79	Chloroplast
10HGO	354	38.44	6.21	hydrophobicity	24.01	25.42	7.34	43.22	Cytosol
G10H	491	55.21	8.81	hydrophilicity	51.32	12.42	6.92	29.33	Chloroplast
GPPS	422	46.34	6.04	hydrophilicity	57.82	4.98	3.55	33.65	Chloroplast

AA represents amino acid, PI represents theoretical isoelectric point, MW represents Molecular weight.

Using NCBI database to compare plant homologous proteins. The amino acids encoded by RgDXS have more than 90% similarity with *Salvia splendens*, *Sesamum indicum*, *Salvia officinalis*. The amino acids encoded by RgDXR have more than 80% similarity with *Handroanthus impetiginosus*, *Osmanthus fragrans*, *Olea europaea var. sylvestris*. The amino acid encoded by Rg10HGO, RgG10H and RgGPPS has the highest similarity with *Striga asiatica*(80.74%), *Phtheirospermum japonicum*(92.81%) and *Sesamum indicum*(90.07%), respectively (Fig. S2). In addition, build the Phylogenetic tree of DXS, 10HGO, G10H and GPPS, *R. glutinosa* and *Scutellaria barbata*, *Striga asiatica*, *Handroanthus impetiginosus*, *Sesamum indicum*, were clustered into one branch, respectively, and DXR branches separately (Fig. S3).

Based on STRING genome, gene co-occurrence on DXS, DXR, 10HGO, G10H, GPPS synthase of *R. glutinosa* was analyzed, found that they were conservative in organisms, occurred in Archaea, Eukaryota and Bacteria, in which they were more conservative in Viridiplantae. Many genes in Viridiplantae appeared to match DXS, DXR, 10HGO, G10H, GPPS synthase of *R. glutinosa*, gene co-occurrence for DXS, DXR, 10HGO, G10H, GPPS of *R. glutinosa*, were all found in 19 species of plants, such as *Aquilegia coerulea*, *Citrus clementine*, *Citrus sinensis*, etc. 4 synthase genes were respectively matched from 9 species of plants, 3 synthase genes were respectively matched from 34 species of plants, and only 1–2 synthase genes in 10 species of plants had co-occurrence, and mainly belong to GPPS. The co-occurrence ratios of DXS, DXR, 10HGO, G10H and GPPS were 87.5%, 94.4%, 38.9%, 30.6% and 90.3%, respectively (Table S2). Further analysis showed that DXS, DXR, 10HGO, G10H and GPPS had high homology in eukaryotes (Table S3, Fig. S4a,b), it has the highest homology with *Erythranthe guttata*, and also has high homology with *Aquilegia coerulea*, *Citrus clementina*, *Citrus sinensis* and *Gossypium raimondii*.

### Expression of *DXS*, *DXR*, *10HGO*, *G10H* and *GPPS*

#### *DXS*

In stage I-IV, the expression of *DXS* in Jinju roots was significantly higher than that in 85 – 5 roots, then was basically the same at stage V, especially in stage IV, Jinjiu expression level was 2-fold that of 85 – 5. In the stage

I-IV, the expression of *DXS* in Jinjiu leaves was significantly higher than that in 85 – 5 leaves, especially in stage IV, Jinjiu expression level was 13-fold that of 85 – 5, but in V stage was lower than 85 – 5 leaves. The overall expression in leaves was higher than that in roots(Fig. 1a).

### ***DXR***

In stage I-III and V, the expression of *DXR* in Jinjiu root was higher than that in 85 – 5 root, but in stage IV was significantly lower than that in 85 – 5 root. In stage IV-V(mature stage), *DXR* in Jinjiu leaf was significantly higher than that in 85 – 5 leaf. The expression level in the leaves of stage IV-V(mature stage) was higher than that in the roots(Fig. 1b).

### ***10HGO***

In stage II-V, the expression of *10HGO* in Jinjiu root was lower than that in 85 – 5, especially in stage V, 85 – 5 expression level was 2-fold that of Jinjiu. In stage IV-V (mature stage), the expression of *10HGO* in Jinjiu leaf was significantly higher than that in 85 – 5 leaf, especially in stage V, Jinjiu expression level was 2-fold that of 85 – 5(Fig. 1c).

### ***G10H***

In stage I-IV, the expression of *G10H* in Jinjiu root was higher than that in 85 – 5 roots, especially in stage III, Jinjiu expression level was 10-fold that of 85 – 5. The expression change in leaves was more complex, In stage IV, the expression of *G10H* in Jinjiu leaves was significantly higher than that in 85 – 5 leaves, while in V stage, lower than that in 85 – 5 leaves. The expression level in leaves was significantly higher than that in roots(Fig. 1d).

### ***GPPS***

In stage II-V, the expression of *GPPS* in Jinjiu root was lower than 85 – 5, especially in stage I V, 85 – 5 expression level was 3-fold that of Jinjiu. The expression of *GPPS* in Jinjiu leaf was significantly lower than that in 85 – 5 leaf except for stage IV(Fig. 1e).

On the whole, gene expression showed variety specificity, tissue specificity and spatio-temporal specificity, in stage IV-V, genes expression is at a higher level in the whole growth cycle, usually reaching a peak in stage IV or V. The expression of *DXS*, *DXR* and *G10H* genes in Jinjiu roots and leaves was more than 85 – 5, while the expression of *10HGO* and *GPPS* genes in Jinjiu roots and leaves was less than 85 – 5, with the maturity of *R.glutinosa*, *DXS* and *G10H* expression showed a trend of increasing at first and then decreasing as a whole, and decreased significantly in stage V, *DXR* *10HGO* and *GPPS* expression decreased at first and then increased, and often continued to increase in stage IV-V.

## **Clustering heat map analysis**

In order to study the expression level of genes in 85 – 5 roots, 85 – 5 leaves, Jinjiu roots and Jinjiu leaves in the same period, the expression of *DXS* in 85 – 5 roots was used as control, the expression of each gene was calculated and cluster heat map was drawn,so that to study genes clustering expression.

In stage I, the expression of *DXS* and *G10H* in leaves was higher than roots, Jinjiu leaves was higher than 85 – 5 leaves, Jinjiu roots was higher than 85 – 5 roots, while the expression of *10HGO*, *DXR* and *GPPS* in roots was higher than that in leaves (Fig. 2a), cluster analysis showed that the expressions of *10HGO*, *DXR* and *GPPS* genes were grouped into one group, *DXS* and *G10H* were clustered into one group. In stage II, the expression of *DXS* and *G10H* in leaves was higher than that in roots, and the expression of *DXR*, *10HGO* and *GPPS* in 85 – 5 was higher than that in Jinjiu, cluster analysis showed that the expression of *10HGO*, *DXR* and *GPPS* genes were clustered into one group, and the expression of *DXS* and *G10H* were clustered together (Fig. 2b), and the clustering was the same as that of stage I. In stage III, the expression of *DXS* and *G10H* in leaves was higher than that in roots, Jinjiu leaves was higher than 85 – 5 leaves, Jinjiu roots was higher than 85 – 5 roots, *DXR* in Jinjiu was higher than that in 85 – 5, and *10HGO* and *GPPS* in 85 – 5 was higher than that in Jinjiu (Fig. 2c), cluster analysis showed that the expression of *DXS*, *DXR* and *G10H* was grouped into one group, and *10HGO* and *GPPS* were grouped into one group. In stage IV, the expression of *DXS*, *DXR*, *10HGO*, *G10H* and *GPPS* in leaves was higher than that in roots, and Jinjiu leaves was higher than 85 – 5 leaves, 85 – 5 roots was higher than Jinjiu roots (Fig. 2d), cluster analysis showed that the expression of *10HGO*, *DXR* and *G10H* was clustered into one group, *DXS* and *GPPS* was clustered into one group. In stage V, the expression of *DXS*, *DXR*, *10HGO*, *G10H* and *GPPS* in leaves was higher than that in roots, and the expression was more complex, cluster analysis showed that *DXR* and *GPPS* gene expression were clustered into one group, *DXS* and *G10H* gene expression were clustered into one group, and *10HGO* was a separate group (Fig. 2e).

## Accumulation dynamics of iridoid glycosides

### Different varieties

In roots, the content of total iridoid glycosides of 85 – 5 and Jinjiu reached the highest in stage IV and decreased in stage V, and in the mature stage of *R. glutinosa* (IV-V), the content of iridoterpene glycosides in Jinjiu roots was significantly higher than that in 85 – 5 roots. In leaves, the content of total iridoid glycosides of 85 – 5 and Jinjiu reached the highest in stage III and decreased continuously in stage IV-V, in mature stage (IV-V stage), Jinjiu leaves was significantly lower than that in 85 – 5 leaves. Further comparison showed that the content of total iridoid glycosides in leaves was higher than that in roots in the early growth stage (I-II stage), from the middle growth stage (III stage), the content of roots was higher than that in leaves, and it was also the same in the later growth stage (IV-V stage) (Fig. 3a). It is worth noting that the content of iridoid glycosides in Jinjiu root was significantly higher than that in 85 – 5 roots in the mature stage (IV-V stage).

### Different producing areas

In roots, the content of total iridoid glycosides in Wenxian was the highest in stage III, and that in Xinxiang was the highest in stage IV, in the mature stage (IV-V stage), the content of total iridoid glycosides in Wenxian root was lower than that in Xinxiang root. In leaves, the content of total iridoid glycosides in Wenxian and Xinxiang reached the highest in stage III, decreased continuously in stage IV-V, and in mature stage (IV-V), Wenxian leaves was slightly lower than that in Xinxiang leaves. Further comparison showed that in the early growth stage (I-II stage), the content of total iridoid glycosides in leaves was higher than that in roots, but from the middle growth stage (III stage), Wenxian root increased significantly, then in stage IV, Xinxiang root increased significantly, but both decreased in stage V (Fig. 3b). It is worth noting that in stage V, the content of iridoid glycosides in Wenxian root was almost the same as that in Xinxiang root.

## Analysis of the correlation between iridoid glycoside accumulation and gene expression

*R. glutinosa* uses roots as medicine, we use Jinjiu root and 85 – 5 root as research materials, SPSS17.0 software to analyze the correlation between iridoid glycoside accumulation and related enzyme genes expression. The results showed that there was a significant negative correlation between the content of total iridoid glycosides and the expression of *GPPS* in 85 – 5 roots, and the correlation coefficient was  $-0.906 (P \leq 0.05)$ , and there was no significant correlation with *DXS*, *DXR*, *10HGO* and *G10H*. In Jinjiu roots, the content of total iridoid glycosides was significantly negatively correlated with the expression of *DXR*, and the correlation coefficient was  $-0.991 (P \leq 0.01)$ , and there was no significant correlation with *DXS*, *GPPS*, *10HGO* and *G10H* (**Table S4**).

### Level of Genomic Methylation in *R. glutinosa*

With the growth of *R. glutinosa*, the content of 5mC in roots and leaves reached the maximum in stage III, and decreased continuously in stage IV-V, and the content of 5mC in leaves was higher than that in roots during the whole growth cycle (**Fig. S5**). Without changing the methylation status of the restriction site, the methylation state of DNA sequence can be detected by using *HpaII* and *MspI* with different sensitivity to CCGG methylation. *HpaII* is not sensitive to the full methylation (double-stranded methylation) of single or two cytosines and only cleaves hemimethylation, while *MspI* is sensitive to fully methylated internal cytosine and insensitive to fully methylated external cytosine. Therefore, the MSAP analysis of the restriction fragment can reflect the degree and status of methylation of the enzyme site. In this study, the band patterns measured by MSAP method are divided into I, II, III and IV, 4 species. I: Both H and M have bands and no methylation occurs (**Fig. S6a**); II: *HpaII* has bands and *MspI* no bands, external methylation of single-stranded DNA (**Fig. S6b**); III: *HpaII* no bands and *MspI* has bands, internal methylation of double-stranded DNA (**Fig. S6c**); IV: MSAP could not detect the complete methylation sites of cytosine (mCCGG/GGCmC or mCmCCGG/GGmCmC) on the outside or inside and outside of DNA, so H and M had no bands at this site, and the band pattern in this case was expressed by IV.

We used two groups of restriction endonuclease digestion combinations of *EcoRI* and *MspI*, *EcoRI* and *HpaII*, among the 48 pairs of primer combinations, 6 pairs of primer combinations were selected, resulting in 39 polymorphic loci, and the bands were statistically analyzed after selective amplification.

In roots, six pairs of primers amplified about 60–84 clear bands, of which the number of methylated bands was 24–106, accounting for 44.44%-60.00%, and the proportion of total methylation bands was 20.99%-27.14%, indicating that most of the genomic CCGG sequences in *R. glutinosa* roots are in a state of hemimethylation and full methylation (**Table S5**). In leaves, six pairs of primers amplified about 73–99 clear bands, of which the number of methylated bands was 40–56 bands, accounting for 46.46%-60.22%, and the proportion of total methylation bands was 21.21%-30.11%, indicating that most of the genomic CCGG sequences in *R. glutinosa* leaves are in a state of hemimethylation and full methylation (**Table S6**). Further analysis showed that the total methylation ratio of roots reached the highest in stage II, reaching 27.14%, and stages II, IV and V were basically the same (27.14%, 26.87%, 26.67%), and the ratio of leaves reached the highest in stage V, reaching 30.11%, both roots and leaves show the trend of decreasing first and then increasing (**Fig. 4a**). The ratio of methylated bands of roots reached the highest in stage V, reaching 60.00%, and there was little difference in II-V (58.57%, 58.33%, 56.72%, 60.00%), and the ratio of leaves reached the highest in stage V, reaching 60.22%, and there was little difference between stage IV and V (57.53%, 60.22%), both roots and leaves show the trend of decreasing first and then increasing (**Fig. 4b**).

### Effects of 5-azaC on accumulation of iridoid glycosides in *R. glutinosa*

The content of total iridoid glycosides in 85 – 5 roots accumulated continuously with the increase of growth period, after treatment with 5-azaC, content of iridoid glycosides increased significantly, in the same growing period, the content of total iridoid glycosides increased with the increase of 5-azaC concentration, especially in the mature stage (IV-V), high concentration is more significant (100 $\mu$ M or 250 $\mu$ M). It is worth noting that in stage III, 250 $\mu$ M 5-azaC significantly inhibited the synthesis of iridoid glycosides (Fig. 5a). The content of total iridoid glycosides in 85 – 5 leaves was more complicated. In stage I, II, III, V, different concentrations of 5-azaC had no significant effect on the accumulation of total iridoid glycosides, only in stage IV, 5-azaC has obvious promotion effect. It is worth noting that in stage II and V, low concentration of 5-azaC (15 $\mu$ M-100 $\mu$ M) significantly inhibited the synthesis of iridoid glycosides (Fig. 5b).

In Jinjiu roots, 5-azaC promoted the accumulation of iridoid glycosides during the whole growth cycle, in the early growth stage (I-II stage) of *R.glutinosa*, the accumulation of iridoid glycosides at different concentrations of 5-azaC was very significant, but in the middle growth stage (III stage) showed inhibitory effect, then in the late growth stage (IV-V stage), it showed a promoting effect but was not significant (Fig. 5c). The content of total iridoid glycosides in Jinjiu leaves was more complicated. In general, 5-azaC promoted the accumulation of iridoid glycosides, and in stage III, IV, V, promoting effect of low concentration and high concentration was significant, but middle concentration was not significant (Fig. 5d).

### Effects of 5- 5-azac on gene expression in *R.glutinosa*

After treatment with different concentrations of 5-azaC, we detected the changes of *DXS*, *DXR*, *10HGO*, *G10H* and *GPPS* expression.

In 85 – 5 roots, 5-azaC promoted the expression of *DXS*, *DXR*, *10HGO*, *G10H* and *GPPS* in varying degrees, with the increase of 5-azaC concentration, the promoting effect increased at first and then decreased, the promoting effect of 15–50 $\mu$ M 5-azaC was better than other concentration, when the concentration of 5-azaC was more than 100 $\mu$ M, it inhibited the expression as a whole. It is worth noting that the expression of *G10H* in stage IV, 30 $\mu$ M 5-azaC treatment was nearly 5 times higher than that in the control group, and that of *GPPS* in stage III, 50 $\mu$ M 5-azaC treatment was nearly 6 times higher than that in the control group (Fig. 6a). In Jinjiu roots, different concentrations of 5-azaC significantly inhibited the expression of *DXS*, which decreased at first and then enhanced with the increase of concentration, and 5-azaC promoted the expression of *DXR*, *10HGO* and *GPPS* to a certain extent, especially in the stage I-II, both low concentration (15 $\mu$ M, 30 $\mu$ M) and high concentration (100 $\mu$ M, 250 $\mu$ M) significantly promoted the expression. 5-azaC promoted the expression of *G10H* in varying degrees, with the increase of 5-azaC concentration, the promoting effect of *G10H* increased at first and then decreased, 30–50 $\mu$ M 5-azaC has great promoting effect, and when the concentration of 5-azaC was more than 100 $\mu$ M, inhibition of expression. It is worth noting that in stage IV, the expression of *DXS* under different concentrations of 5-azaC was more than 10 times lower than that of the control group, the expression of *DXR* in stage II, 250 $\mu$ M 5-azaC was nearly 6 times higher than that of the control group, and the expression of *G10H* in stage II, 50 $\mu$ M 5-azaC treatment was nearly 10 times higher than that of the control group (Fig. 6b).

In 85 – 5 leaves, 5-azaC promoted the expression of *DXS*, *DXR*, *10HGO*, *G10H* and *GPPS* in varying degrees, and the promoting effect increased at first and then decreased with the increase of 5-azaC concentration, and promoting effect of 15–50 $\mu$ M 5-azaC was better, when the concentration of 5-azaC was more than 100 $\mu$ M, the promoting effect was not as significant as that of low concentration. It is worth noting that the expression of

*GPPS* in stage III, 50 $\mu$ M 5-azaC treatment was nearly 6 times higher than that of the control group, while that of *G10H* in stage II, treated with various concentrations of 5-azaC was more than 4 times lower than that of the control group, and in stage IV, the expression level of *G10H* treated with 30 $\mu$ M 5-azaC was 5 times lower than that of the control group (Fig. 6c). In Jinjiu leaves, 5-azaC promoted the expression of *DXS*, *DXR*, *10HGO*, *G10H* and *GPPS* in varying degrees, with the increase of 5-azaC concentration, the promoting effect increased at first and then decreased. The promoting effect of 15–50 $\mu$ M 5-azaC was better, when the concentration of 5-azaC was more than 100 $\mu$ M, the promoting effect was not as significant as that of low concentration. It is worth noting that the expression of *DXS* in stage III and IV was lower than that in the control group under all concentrations of 5-azaC, while the promoting effect of *DXR* in stage II was very significant, especially at 30 $\mu$ M and 100 $\mu$ M, it increased by 14 and 25 times, respectively (Fig. 6d).

### Effects of 5-azaC on 5mC Content in Genomic DNA of *R. glutinosa*

We used different concentrations of 5-azaC to treat roots and leaves, and found that with the maturity of *R. glutinosa*, the content of genomic 5mC in roots and leaves in mature stage was significantly higher than that in seedling stage, and the content of genomic DNA 5mC in roots and leaves decreased with the increase of 5-azaC concentration, 5-azaC significantly inhibited the formation of genomic methylation in roots and leaves (Fig. 7a,b). In different growth periods, the content of 5mC in the control group was the highest, and the inhibitory effect gradually enhanced with the increase of 5-azaC concentration in the same growth period, further analysis showed that the content of genomic 5mC in *R. glutinosa* root and leaf was different at the same period, and leaf was higher than that in root tuber.

### Effect of 5-azaC on the level of Genomic Methylation

In roots, 6 pairs of primers amplified about 61–146 clear bands, of which the number of methylated bands was 31–80 bands, accounting for 45.63%-76.29%, and the proportion of fully methylated bands was 16.98%-39.02%, indicating that most of the genomic CCGG sequences in *R. glutinosa* roots are in a state of hemimethylation and total methylation (Table S7). The total methylation ratio of the control group was significantly lower than that of the treatment group except stage II, and increased at first and then decreased with the increase of 5-azaC concentration (Fig. 8a). The change of methylation band ratio (MSAP%) is more complex, MSAP% of the control group in stage I is slightly lower than that in the other four stages, and there is no significant difference in the other four stages, on the whole, MSAP% of 5-azaC treatment in the same growth period is basically higher than that of the control group, and the maximum value of 15 $\mu$ M-100 $\mu$ M concentration treatment appeared in stage IV, IV, IV and V, respectively, and the maximum value of 250 $\mu$ M concentration treatment appeared in stage II (Fig. 8b).

In leaves, 6 pairs of primers amplified about 61–130 clear bands, of which the number of methylated bands was 24–83 bands, accounting for 33.33%-68.03%, and the proportion of fully methylated bands was 13.04%-35.29%, indicating that most of the genomic CCGG sequences in *R. glutinosa* leaves are in a state of hemimethylation and total methylation (Table S8). The change of total methylation ratio in leaves was more complex, low concentration of 5-azaC in the same growth period played a promoting role, while high concentration of 5-azaC played an inhibitory role, the control group reached the maximum value in stage III, the maximum value of 15 $\mu$ M-100 $\mu$ M concentration treatment appeared in II, III, III and II stage, and the maximum value of 250 $\mu$ M concentration treatment appeared in V stage (Fig. 8c). Under the treatment of 5-azaC, in I-III stage, the methylation band ratio (MSAP%) was promoted at low concentration, inhibited at high concentration,

but both inhibited in IV and V stage. The control group reached the maximum value in stage IV, and the maximum value of 15 $\mu$ M-250 $\mu$ M concentration treatment appeared in stage II, III, IV, II and III, respectively (Fig. 8d).

### **Change of Methylation Status in *R. glutinosa* treated with 5-azaC**

We used roots and leaves of mature *R. glutinosa* to analyze changes in DNA methylation status. Compared with the control group, the changes of genomic methylation status of *R. glutinosa* treated with 5-azaC could be divided into 3 categories and 12 bands. We set class A as a monomorphic band, means that the control group has the same methylation sites as the treatment group, indicating that the methylation status of CCGG sites remains unchanged, while B and C are polymorphic bands, means that methylation sites in the control and treatment groups were different, type B is methylation increased band pattern, indicating that the methylation level of genomic DNA has increased, and the band pattern of DNA methylation increase can be summarized as follows: I $\rightarrow$ III, I $\rightarrow$ IV, II $\rightarrow$ III, II $\rightarrow$ IV. Type C is the demethylation type, which indicates that the methylation level of genomic DNA has decreased, and the band pattern of demethylation change is: IV $\rightarrow$ II, IV $\rightarrow$ I, III $\rightarrow$ II, III $\rightarrow$ I. Due to the limitation of MSAP technique, the increase or decrease of DNA methylation could not be determined as I $\rightarrow$ II, III $\rightarrow$ IV, IV $\rightarrow$ III, II $\rightarrow$ I.

Statistical analysis of genomic DNA methylation increases and decreases in the band pattern (Table 3), we found that in roots most of the bands with increased methylation were II $\rightarrow$ IV, which changed from semi-methylation to full methylation, and a few transformed bands were I $\rightarrow$ III, at the concentration of 30 $\mu$ M-100 $\mu$ M 5-azaC, the methylation band increased significantly. The demethylation band type is mainly IV $\rightarrow$ II, with the increase of 5-azaC concentration, the number of demethylated bands also increased, and reached the maximum value of 12 bands at 50 $\mu$ M, III $\rightarrow$ I and IV $\rightarrow$ I also account for a certain proportion of demethylated bands, and as the concentration increased, the number of demethylated bands also increased and all reached the maximum value at 250 $\mu$ M. Further analysis we found that the number of methylation sites decreased more than the number of methylation sites increased, which was consistent with the trend of MSAP% under 5-azaC treatment in stage V.

Table 3  
DNA methylation pattern of *Rehmannia* root under 5-azaC

Type of methylation pattern	Band Type				Number of sites				
	CK		Treat		Root				
	H	M	H	M	CK- 15μM	CK- 30μM	CK- 50μM	CK- 100μM	CK- 250μM
B1(I→III)	1	1	0	1	0	2	1	1	0
B2(II→III)	1	0	0	1	1	0	0	0	0
B3(II→IV)	1	0	0	0	2	5	6	4	2
B4(I→IV)	1	1	0	0	0	0	0	0	0
C1(III→I)	0	1	1	1	3	3	6	8	9
C2(III→II)	0	1	1	0	0	0	0	1	0
C3(IV→II)	0	0	1	0	4	9	12	9	9
C4(IV→I)	0	0	1	1	0	0	2	7	8

The methylation increase band pattern and demethylation band pattern in leaves are more than those in roots (Table 4), we found that in leaves most of the bands with increased methylation were II→IV, which changed from semi-methylation to full methylation, and a few transformed bands were I→III, at the concentration of 30μM-50μM 5-azaC, the methylation band increased significantly. The demethylation band type is mainly IV→II, with the increase of 5-azaC concentration, the number of demethylated bands also increased, and reached the maximum value of 16 bands at 250μM, III→I, III→II and IV→I also account for a certain proportion of demethylated bands, and as the concentration increased, the number of demethylated bands also increased and all reached the maximum value at 250μM also. Further analysis we found that the number of methylation sites decreased more than the number of methylation sites increased, especially under high concentration treatment, the number of bands decreased significantly, which was consistent with the trend of MSAP% under 5-azaC treatment in stage V.

Table 4  
DNA methylation pattern of *Rehmannia* leaf under 5-azaC

Type of methylation pattern	Band Type				Number of sites				
	CK		Treat		Leaf				
	H	M	H	M	CK- 15μM	CK- 30μM	CK- 50μM	CK- 100μM	CK- 250μM
B1(I→III)	1	1	0	1	0	3	2	2	0
B2(II→III)	1	0	0	1	1	0	0	0	0
B3(II→IV)	1	0	0	0	3	5	7	3	2
B4(I→IV)	1	1	0	0	0	0	0	0	0
C1(III→I)	0	1	1	1	4	4	8	9	10
C2(III→II)	0	1	1	0	0	0	0	1	0
C3(IV→II)	0	0	1	0	5	7	10	13	16
C4(IV→I)	0	0	1	1	0	0	3	6	8

In general, the number of methylated and demethylated bands increased with the increase of 5-azaC concentration in roots and leaves of *R. glutinosa*, and effects of 5-azaC on genomic methylation status of roots and leaves were roughly the same.

## Discussion

Plant secondary metabolites play an important role in many aspects of plant life activities such as affecting plant growth and development, adapting to the environment, resisting diseases and insect pests [40–42]. There are many factors affecting the accumulation of secondary metabolites in plants, such as temperature, light, water, nutrients and so on [43–46]. The metabolic pathway of terpenoids is very complex, involving a variety of enzymes and genes, and some studies have shown that the accumulation of secondary metabolites is regulated by epigenetics. In this study, we used *R. glutinosa* 85 – 5 and Jinjiu as experimental materials and found that in the early growth stage (I-II stage), the clustering of gene expression is the same (Fig. 2a,b), which reveals the level and clustering trend of genes expression in different tissues in the early stage growth, and in the middle growth stage (III stage), the clustering of gene expression is similar to that in stage I and II, but in the later growth stage (IV-V stage), it is obviously that the clustering of gene expression has changed significantly (Fig. 2c,d,e), although the expression of gene clusters varied in different growth stages, the expression of genes in the late growth period was higher than that in the early growth period, meanwhile, we found that the accumulation of iridoid glycosides also presents an upward trend, which was similar to the genes expression, this results indicated that the level of gene expression affected the accumulation of iridoid glycosides, but the correlation analysis showed that there was no significant positive correlation between the accumulation of iridoid glycosides and gene expression, we speculate that this is due to the fact that the

accumulation of iridoid glycosides is affected by many internal and external factors, and the *DXS*, *DXR*, *10HGO*, *G10H*, *GPPS* in this study are only part of the genes in the metabolic pathway, so further study is needed.

DNA methylation plays an important role in the growth and development of plants and the accumulation of secondary metabolites, we found that the ratio of total methylation and the ratio of methylated bands (MSAP%) in the roots increased gradually with the maturity of *R. glutinosa*, and leaves are similar to roots, and it was consistent with gene expression and accumulation of iridoid glycosides, total methylation% and MSAP% reached the maximum in stage IV or V, while the gene expression usually reached the maximum in stage III or IV, indicating that proper methylation had little effect on gene expression in the early stage of *R. glutinosa* growth, while the methylation site continued to increase in the later stage, resulting in the inhibition of gene expression.

We also found that DNA methylation and demethylation affect the accumulation of secondary metabolites and the expression of related genes in the secondary metabolic pathway. In this study, different concentrations of 5-azaC can promote the accumulation of iridoid glycosides to a certain extent, and the promoting effect of low concentration is not as significant as that of high concentration, and the promoting effect is usually the most significant when the concentration is 100 $\mu$ M and 200 $\mu$ M, and different concentrations of 5-azaC also can promote *DXS*, *DXR*, *10HGO*, *G10H*, *GPPS* expression. Interestingly, in the II stage of 85 – 5 roots, when the concentration of 5-azaC was 15 $\mu$ M and 50 $\mu$ M, the gene expression was inhibited, and the accumulation of iridoid glycosides was also inhibited. In the II, III, V stage of 85 – 5 leaves, gene expression and iridoid glycoside accumulation were inhibited by 5-azaC treatment, so it can be inferred that the effects of 5-azaC on the accumulation of iridoid glycosides and gene expression were consistent, and the increase of gene expression leads to an increase in the accumulation of iridoid glycosides, and vice versa.

The use of 5-azaC will lead to changes in the methylation status of genomic DNA, and affects the normal growth and development of plants [47, 48] and the accumulation of metabolites. The Research found that 5-azaC inhibited the formation of genomic DNA methylation, and the inhibition became more significant with the increase of concentration, further analysis of total methylation ratio and methylation band ratio (MASP%), we found that low concentration of 5-azaC promotes the formation of methylation, and high concentration of 5-azaC inhibits the formation of methylation. Interestingly, the formation of methylation sites and demethylation in roots by 5-azaC treatment were less significant than those in leaves, and the change of complete methylation ratio is more significant than methylation band ratio, in order to verify these phenomena, we statistically analyzed the dynamic changes of methylation state under 5-azaC treatment, found that no matter the methylation increase band pattern or the methylation decrease band pattern, the number in the roots is less than that in the leaves, and the number of methylation sites increased and decreased the most when the concentration of 5-azaC was 50 $\mu$ M or 100 $\mu$ M in roots, and 250 $\mu$ M in leaves. In roots, the increased methylation band pattern is mainly the transition from semi-methylation to total methylation, the demethylation bands are mainly characterized by the transition from total methylation to semi-methylation, and the transformation from total methylation to non-methylation also accounts for a considerable proportion, and this situation in the leaves is similar to the roots, these corresponds to the above research results. Further analysis showed that with the increase of 5-azaC concentration, the number of demethylation sites increased gradually, when treated with low concentration(15 $\mu$ M-50 $\mu$ M) of 5-azaC, proper demethylation promoted gene expression, and the accumulation of iridoid glycosides was also promoted, while high concentration(100 $\mu$ M-250 $\mu$ M) 5-azaC treatment led to excessive demethylation, which affected the normal gene expression, but the accumulation of

iridoid glycosides was still promoted, and in some cases, the promoting effect of high concentration was more significant than that of low concentration, we speculate that this is because the synthesis process of iridoid glycosides is complex, and there are many enzymes and genes involved, so there is no significant correlation only from the results of this study, and further research is needed, and under different concentrations of 5-azaC treatment, the dynamic changes of iridoid glycoside accumulation, gene expression and methylation status in mature leaves were more complex and obvious than roots, shows that the treatment of 5-azaC is tissue specific and plays a more significant role in leaves. Therefore, we concluded that 5-azaC inhibited the methylation of genomic DNA, promoted the expression of related enzyme genes in the iridoid glycoside synthesis pathway, and promoted the accumulation of iridoid glycosides.

## Conclusion

We compared the iridoid glycoside accumulation, gene expression and genomic DNA methylation of *R.glutinosa* between the control group and the 5-azaC treatment group, and found that with the maturity of *R.glutinosa*, iridoid glycosides gradually accumulated, gene expression and methylation sites increased, after treatment with different concentrations of 5-azaC, iridoid glycoside accumulation and gene expression were promoted, and DNA methylation was inhibited. Through analyzing the dynamic changes among these, it is expected to reveal the correlation between DNA methylation and iridoid glycoside accumulation and the expression of key enzyme genes in iridoid glycoside metabolic pathway, which is expected to provide reference for revealing the mechanism of plant secondary metabolic pathways from the perspective of epigenetics.

## Declarations

### Ethics approval and consent to participate

We confirm that all materials and methods were in compliance with relevant institutional, national, and international guidelines and legislation.

### Consent for publication

Not applicable.

### Availability of data and materials

All data generated or analysed during this study are included in this published article [and its supplementary information files].

### Competing interests

The authors declare that they have no competing interests.

### Funding

This research was supported by NSFC (National Science Foundation of China) (No. 31870312 and No.31500262), Henan Natural Science Foundation (17HASTIT034) and Fund of Henan Normal University (2019JQ01).

## Authors' contributions

LYK and LCH collected *Rehmannia glutinosa* seeds and planted in the field. DTY, WXY, QQT and CPL performed the experiments, analyzed and interpreted the data and prepared figures, DTY performed data analysis and wrote the manuscript. DHY and ZYQ revised the article critically. All authors have read and approved the manuscript.

## Acknowledgments

Not applicable.

## Statement

Collection of *Rehmannia glutinosa* in this research materials conforms to and complies with the IUCN Policy Statement on Research Involving Species at Risk of Extinction and the Convention on the Trade in Endangered Species of Wild Fauna and Flora. In addition, according to the List of National Key Protected Wild Plants issued by the State Forestry and Grassland Bureau of China, *Rehmannia glutinosa*, the experimental material of this study, is neither a national key protected wild plant nor an endangered plant species.

College of Life Sciences, Henan Normal University, Xinxiang, HeNan, China

Corresponding author: Hongying Duan

12, April, 2021

## References

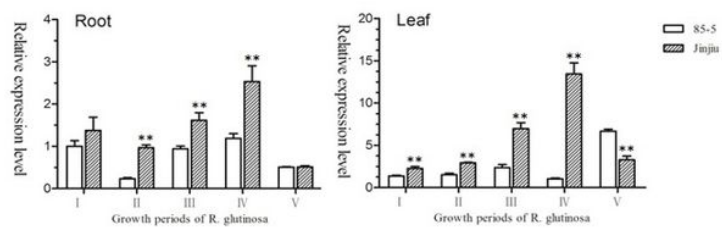
1. Wang LJ, Fang X, Yang CQ, Li JC, Chen XY. Biosynthesis and regulation of secondary terpenoid metabolism in plants. *SCIENTIA SINICAVitae*. 2013;43(12):1030–1046. [https:// doi.org/10.1360/052013-307](https://doi.org/10.1360/052013-307).
2. Pu XJ, Dong XM, Li Q, Chen ZX, Liu L. An update on the function and regulation of MEP and MVA pathways and their evolutionary dynamics. *J Integr Plant Biol*. 2021; [https:// doi.org/ 10.1111/jipb.13076](https://doi.org/10.1111/jipb.13076).
3. Li H, Yang SQ, Wang H, Tian J, Gao WY. Biosynthesis of the iridoid glucoside, lamalbid, in *Lamium barbatum*. *Phytochemistry*. 2010;71(14-15):1690-1694. [https:// doi.org/10.1016/j.phytochem.2010.06.019](https://doi.org/10.1016/j.phytochem.2010.06.019).
4. Choi CS, Sano H. Abiotic-stress induces demethylation and transcriptional activation of a gene encoding a glycerophosphodiesterase-like protein in tobacco plants. *Mol Genet Genomics*. 2007;277(5):589-600. [https:// doi.org/10.1007/s00438-007-0209-1](https://doi.org/10.1007/s00438-007-0209-1).
5. Liu Y, Luo SH, Schmidt A, Wang G, Sun G, Grant M, Kuang Ce, Yang M, Jing SX, Li CH, Schneider B, Gershenzon J, Li S. A Geranyl farnesyl Diphosphate Synthase Provides the Precursor for Sesterterpenoid (C-25) Formation in the Glandular Trichomes of the Mint Species *Leucosceptrum canum*. *Plant Cell*. 2016;28: 804-822. [https:// doi.org/10.1105/tpc.15.00715](https://doi.org/10.1105/tpc.15.00715).
6. Rohmer M, Knani M, Simonin P, Sutter B, Sahm H. Isoprenoid biosynthesis in bacteria: a novel pathway for the early steps leading to isopentenyl diphosphate. *Biochem J*. 1993;295:517. [https:// doi.org/10.1006/bbrc.1993.2277](https://doi.org/10.1006/bbrc.1993.2277).

7. Rohmer M. The discovery of a mevalonate-independent pathway for isoprenoid biosynthesis in bacteria, algae and higher plants. *Nat prod rep.* 1999;16:565-574. [https:// doi.org/10.1039/A709175C](https://doi.org/10.1039/A709175C).
8. Zhao LS, Chang WC, Xiao YL, Liu HW, Liu PH. Methylerythritol Phosphate Pathway of Isoprenoid Biosynthesis. *Annu Rev Biochem.* 2013;82:497. [https:// doi.org/10.1146/annurev-biochem-052010-100934](https://doi.org/10.1146/annurev-biochem-052010-100934).
9. Geu-Flores F, Sherden NH, Courdavault V, Burlat V, Glenn WS, Wu C, Nims E, Cui YH, Sarah E, Connor O. An alternative route to cyclic terpenes by reductive cyclization in iridoid biosynthesis. *Nature.* 2012; 492(7427):138-142. [https:// doi.org/10.1038/nature11692](https://doi.org/10.1038/nature11692).
10. Wu XY, Liu XL. Progress of Biosynthetic Pathway and the Key Enzyme Genes of Iridoids. *Chinese J Ethnomedicine Ethnopharmacy.* 2017;26:44-48. [https:// doi.org/CNKI:SUN:MZMJ.0.2017-08-013](https://doi.org/CNKI:SUN:MZMJ.0.2017-08-013).
11. Burlat V, Oudin A, Courtois M, Rideau M, St-Pierre B. Co-expression of three MEP pathway genes and geraniol 10-hydroxylase in internal phloem parenchyma of *Catharanthus roseus* implicates multicellular translocation of intermediates during the biosynthesis of monoterpene indole alkaloids and isoprenoid-derived primary metabolites. *The Plant Journal.* 2004;38(1):131-141. <https://doi.org/10.1111/j.1365-313X.2004.02030.x>.
12. Sprenger GA, Schörken U, Wiegert T, Grolle S, Graaf AAD, Taylor SV, Begley TP, Bringer MS, Sahm H. Identification of a thiamin-dependent synthase in *Escherichia coli* required for the formation of the 1-deoxy-D-xylulose 5-phosphate precursor to isoprenoids, thiamin, and pyridoxol. *P NATL ACAD SCI USA.* 1997; 94(24): 12857-12862.
13. Mandel MA, Feldmann KA, Herrera EL, Rocha SM, Leon P. CLA1, a novel gene required for chloroplast development, is highly conserved in evolution. *Plant Journal.* 1996;9(05): 649-658. <https://doi.org/10.1046/j.1365-313X.1996.9050649.x>.
14. Estevez M, Cantero A, Reindl A, Reichler S, Leon P. 1-Deoxy-D-xylulose-5-phosphate synthase, a limiting enzyme for plastidic isoprenoid biosynthesis in plants. *Journal of Biological Chemistry.* 2001;276(25): 22901-22909. <https://doi.org/10.1074/jbc.M100854200>.
15. Carretero-Paulet L. Expression and Molecular Analysis of the Arabidopsis DXR Gene Encoding 1-Deoxy-d-Xylulose 5-Phosphate Reductoisomerase, the First Committed Enzyme of the 2-C-Methyl-d-Erythritol 4-Phosphate Pathway. *Plant Physiol.* 2002;129(4):1581-1591. [https://doi.org/ 10.1104/pp.003798](https://doi.org/10.1104/pp.003798).
16. Lichtenthaler, Hartmut K. THE 1-DEOXY-D-XYLULOSE-5-PHOSPHATE PATHWAY OF ISOPRENOID BIOSYNTHESIS IN PLANTS. *Plant.Molecular Biology.* 1999;50(1):47-65. <https://doi.org/10.1146/annurev.arplant.50.1.47>.
17. Wang CH, Lei XY, Xia J, Wang JW. [Effect of down-regulating 1-deoxy-d-xylulose-5-phosphate reductoisomerase by RNAi on growth and artemisinin biosynthesis in \*Artemisia annua\* L.](#) *PLANT GROWTH REGULATION.* 2018;84(3):549-559. <https://doi.org/10.1007/s10725-017-0360-6>.
18. Wang HT, Feng MY, Liang CY, Li WL. Cloning and Expression Analysis of Gene GPPS in Mint. *J Jiangxi Agriculture.* 2013;25: 25-29. [https://doi.org/25\(07\):25-29.0.19386/j.cnki.jxnyxb.2013.07.008](https://doi.org/25(07):25-29.0.19386/j.cnki.jxnyxb.2013.07.008).
19. Xi J, Rossi L, Lin X. Xie DY. Overexpression of a synthetic insect–plant geranyl pyrophosphate synthase gene in *Camelina sativa* alters plant growth and terpene biosynthesis. *Planta.* 2016;244(1):215-230. [https:// doi.org/10.1007/s00425-016-2504-8](https://doi.org/10.1007/s00425-016-2504-8).
20. Schmidt A, Wchtler B, Temp U, Krekling T, Gershenzon J. A Bifunctional Geranyl and Geranylgeranyl Diphosphate Synthase Is Involved in Terpene Oleoresin Formation in *Picea abies*. *Plant Physiol.*

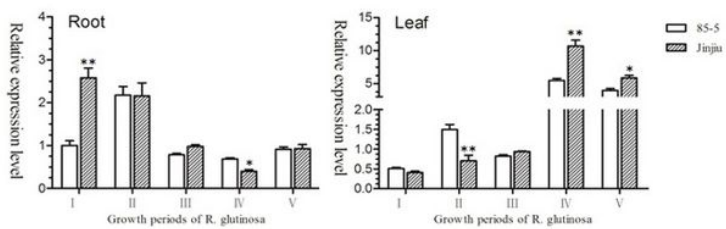
- 2010;152(2): 639-655. <https://doi.org/10.1104/pp.109.144691>.
21. Nagegowda DA, Gutensohn M, Wilkerson CG, Dudareva N. Two nearly identical terpene synthases catalyze the formation of nerolidol and linalool in snapdragon flowers. *Plant Journal*. 2010;55(2):224-239. <https://doi.org/10.1111/j.1365-313X.2008.03496.x>.
22. Zhao B, An ZG, Rausch T, Zu YG. Cloning and Expression of cDNA Encoding Key Enzymes (DXR, SLS, G10H and STR) in Terpene Indole Alkal Biosynthesis Pathway from *Catharanthus roseus*. *Bulletin Botanical Research*. 2007;27(5):564-568. <https://doi.org/10.3969/j.issn.1673-5102.2007.05.013>.
23. Sung PH, Huang FC, Do YY, Huang PL. Functional Expression of Geraniol 10-Hydroxylase Reveals Its Dual Function in the Biosynthesis of Terpenoid and Phenylpropanoid. *J Agric Food Chem*. 2011;59(9):4637-4643. <https://doi.org/10.1021/jf200259n>.
24. Pan Q, Quan W, Yuan F, Xing S, Zhao J, Hae CY, Robert V, Tian Y, Wang G, Tang K. Overexpression of ORCA3 and G10H in *Catharanthus roseus* plants regulated alkaloid biosynthesis and metabolism revealed by NMR-metabolomics. *PLoS One*, 2012;7(8): e43038. <https://doi.org/10.1371/journal.pone.0043038>.
25. Oudin A, Courtois M, Rideau M, Clastre M. The iridoid pathway in *Catharanthus roseus* alkaloid biosynthesis. *Phytochemistry Reviews*. 2007;6(2-3): 259-276. <https://doi.org/10.1007/s11101-006-9054-9>.
26. Verma P, Mathur AK, Srivastava A, Mathur A. Emerging trends in research on spatial and temporal organization of terpenoid indole alkaloid pathway in *Catharanthus roseus*: a literature update. *Protoplasma*. 2012;249(2): 255-268. <https://doi.org/10.1007/s00709-011-0291-4>.
27. Zhang HM, Lang ZB, Zhu JK. Dynamics and function of DNA methylation in plants. *Nat Rev Mol Cell Bio*. 2018;19: 489-506. <https://doi.org/10.1038/s41580-018-0016-z>.
28. Bharti P, Mahajan M, Vishwakarma AK, Bhardwaj J, Yadav SK. AtROS1 overexpression provides evidence for epigenetic regulation of genes encoding enzymes of flavonoid biosynthesis and antioxidant pathways during salt stress in transgenic tobacco. *J Exp Bot*. 2015;66(19): 5959-5969. <https://doi.org/10.1093/jxb/erv304>.
29. Daniel C, Alicia MC, Christopher D, José RS, Matias K, Mariano P, Pablo GM, Isabel A. Overexpression of DEMETER, a DNA demethylase, promotes early apical bud maturation in poplar. *Plant Cell Environ*. 2017; 40(11):2806-2819. <https://doi.org/10.1111/pce.13056>.
30. Zhu HJ, Zhao SJ, Lu XQ, He N, Gao L, Dou JL, Bie ZL, Liu WG. Genome duplication improves the resistance of watermelon root to salt stress. *Plant Physiol Bioch*. 2018; 133:11-21. <https://doi.org/10.1016/j.plaphy.2018.10.019>.
31. Li XL, Yuan J, Dong YS, Fu CH, Li MT, Yu LJ. Optimization of an HPLC Method for Determining the Genomic Methylation Levels of *Taxus* Cells. *J Chromatogr Sci*. 2016;54(2):200-205. <https://doi.org/10.1093/chromsci/bmv129>.
32. Li LQ, Li XL, Fu CH, Zhao CF, Yu LJ. Sustainable use of *Taxus media* cell cultures through minimal growth conservation and manipulation of genome methylation. *Process Biochem*. 2013;48(3):525-531. <https://doi.org/10.1016/j.procbio.2013.01.013>.
33. Li J, Li CL, Lu SF. Systematic analysis of DEMETER-like DNA glycosylase genes shows lineage-specific Smi-miR7972 involved in SmDML1 regulation in *Salvia miltiorrhiza*. *Sci Rep-Uk*. 2018;8(1):7143. <https://doi.org/ARTN7143.10.1038/s41598-018-25315-w>.

34. Jiang L, Li C, Lu S. Identification and characterization of the cytosine-5 DNA methyltransferase gene family in *Salvia miltiorrhiza*. *PeerJ*. 2018;6(17): e4461. <https://doi.org/10.7717/peerj.4461>.
35. Lan LW. Study on the Regulation of DNA Methylation on Ganoderic Acids Biosynthesis in *Ganoderma lucidum*. FuJian Normal University. 2016; Doctoral dissertation.
36. Xia N. Study On The Relationship Between Nitric Oxide-treated Production Of Plant Secondary Metabolite Isoflavone and DNA Methylation. Hefei University of Technology. 2006; Doctoral dissertation.
37. Ni ZJ, Yin LL, Ying QC, Ru YL, Wang DX, Jin L, Xie J, Hu ZJ, Wang HZ, Xu XB. Effects of 5-azaC on bioactive components of dendrobium. *ZheJiang agricultural sciences*. 2014;1(007):1018-1020. <https://doi.org/10.3969/j.issn.0528-9017.2014.07.016>.
38. Duan HY, Li JJ, Wang HN, CheFF, Ding WK, Zhu YQ, Xue Z, Zeng YP, Zhou YQ. Effects of DNA Methylation on Growth and Development of *Rehmannia glutinosa*. *Int J Agric Biol*. 2018; 20:2161-2168. <https://doi.org/10.17957/IJAB/15.0745>.
39. Pieter V, Rene H, Marjo B, Martin R, Theo L, et al. AFLP: a new technique for DNA fingerprinting. *Nucleic Acids Research*. 1995;23:4407-4414. <https://doi.org/10.1093/nar/23.21.4407>.
40. Kim YS, Uefuji H, Ogita S, Sano H. Transgenic tobacco plants producing caffeine: a potential new strategy for insect pest control. *Transgenic Res*. 2006;15(6):667-672. <https://doi.org/10.1007/s11248-006-9006-6>.
41. Hua J, Liu Y, Xiao CJ, Jing SX., Luo SH, Li SH. Chemical profile and defensive function of the latex of *Euphorbia peplus*. *Phytochemistry*. 2017; 136:56-64. <https://doi.org/10.1016/j.phytochem.2016.12.021>.
42. Hectors K, Van Oevelen S, Geuns J, Guisez Y, Jansen MAK, Prinsen E. Dynamic changes in plant secondary metabolites during UV acclimation in *Arabidopsis thaliana*. *Physiol Plantarum*. 2014;152(2):219-230. <https://doi.org/10.1111/ppl.12168>.
43. Salmore AK, Hunter MD. Environmental and Genotypic Influences on Isoquinoline Alkaloid Content in *Sanguinaria canadensis*. *J CHEM ECOL*. 2001;27(9):1729-1747. <https://doi.org/10.1023/A:1010448406809>.
44. Janas KM, Cvikrová M, Pałagiewicz A, Szafranska K, Posmyk MM. Constitutive elevated accumulation of phenylpropanoids in soybean roots at low temperature. *Plant Science*. 2002;163(2):369-373. [https://doi.org/10.1016/S0168-9452\(02\)00136-X](https://doi.org/10.1016/S0168-9452(02)00136-X).
45. Liu Z. Drought-induced in vivo synthesis of camptothecin in *Camptotheca acuminata* seedlings. *Physiologia Plantarum*. 2000;110(4):483-488. <https://doi.org/10.1111/j.1399-3054.2000.1100409.x>.
46. Copley RR, Letunic I, Bork P. Genome and protein evolution in eukaryotes. *CURR OPIN CHEM BIOL*. 2002;6(1):39-45. [https://doi.org/10.1016/S1367-5931\(01\)00278-2](https://doi.org/10.1016/S1367-5931(01)00278-2).
47. Iwase Y, Shiraya T, Takeno K. Flowering and dwarfism induced by DNA demethylation in *Pharbitis nil*. *Physiol Plantarum*. 2010;139(1):118-127. <https://doi.org/10.1111/j.1399-3054.2009.01345.x>.
48. Gao WJ, Li SF, Li ZX, Huang YY, Deng CL, Lu LD. Detection of genome DNA methylation change in spinach induced by 5-azaC. *MOL CELL PROBE*. 2014;28(4):163-166. <https://doi.org/10.1016/j.mcp.2014.02.002>.

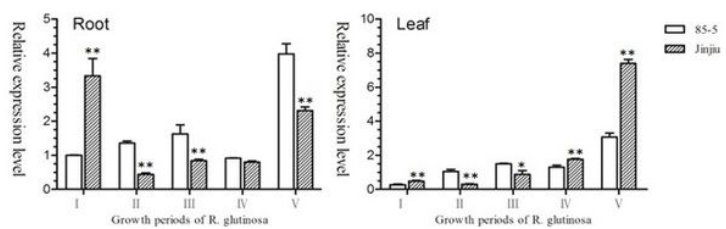
## Figures



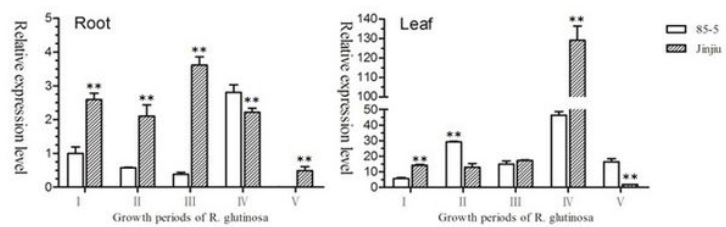
a



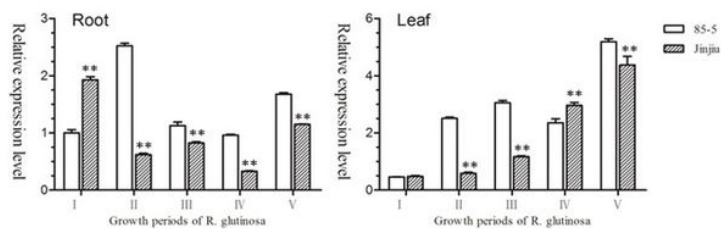
b



c



d



e

**Figure 1**

Relative expression of genes in *R. glutinosa*. a DXS b DXR c 10HGO d G10H e GPPS

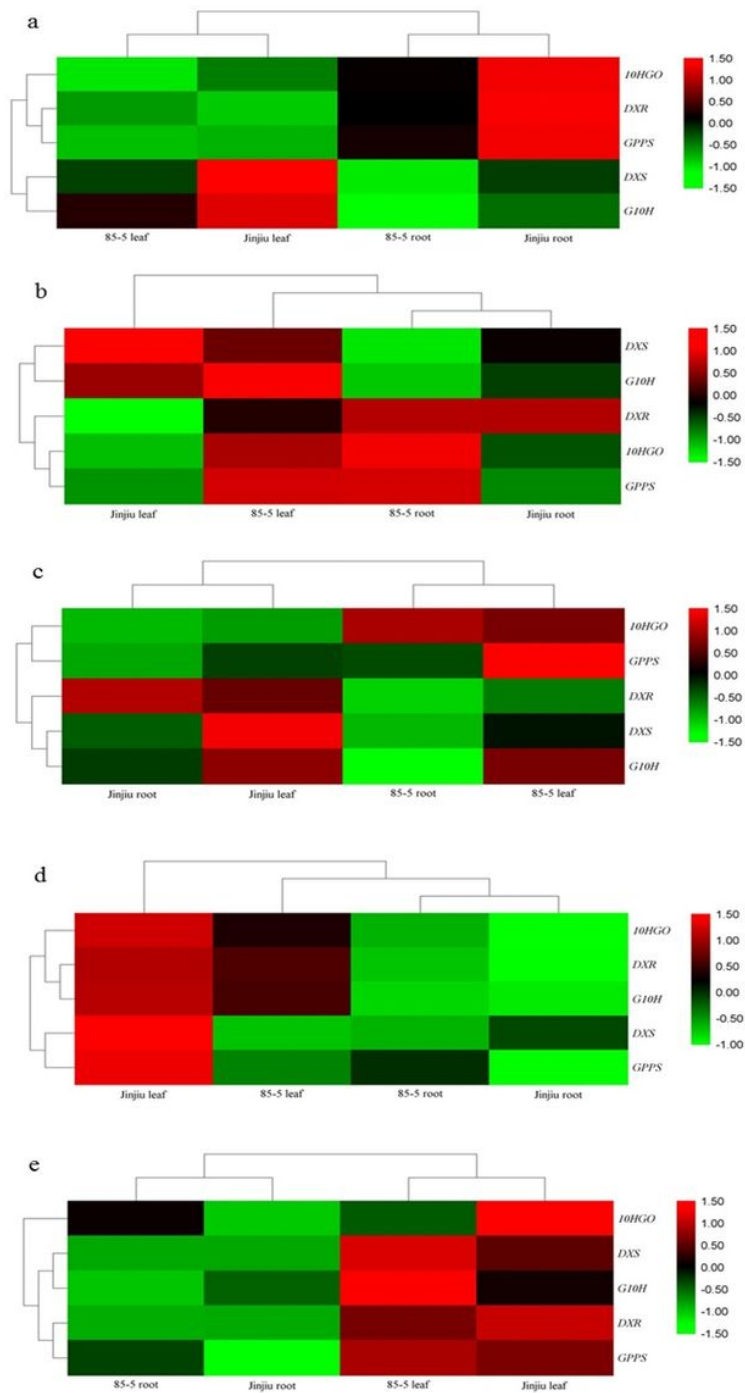


**Figure 2**

Heat map and Cluster analysis of relate enzyme genes in *R. glutinosa*. a: I growth period, b: II growth period, c: III growth period, d: IV growth period, e: V growth period

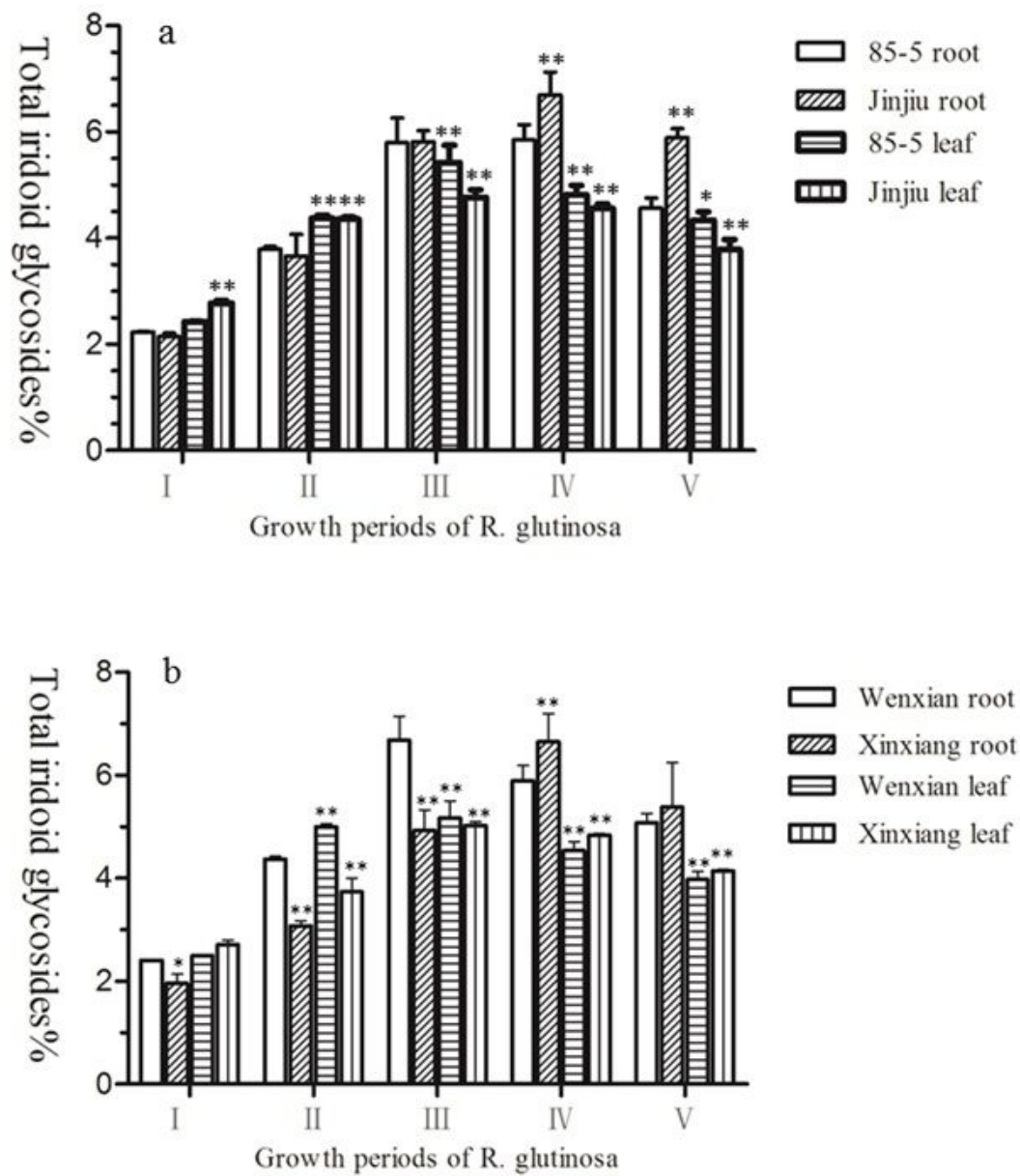


**Figure 3**

Total iridoid glycosides in *R. glutinosa*. a: different varieties; b: different producing areas. statistical significance was determined by a two-sided t-test: \*  $P < 0.05$ , \*\*  $P < 0.01$ .

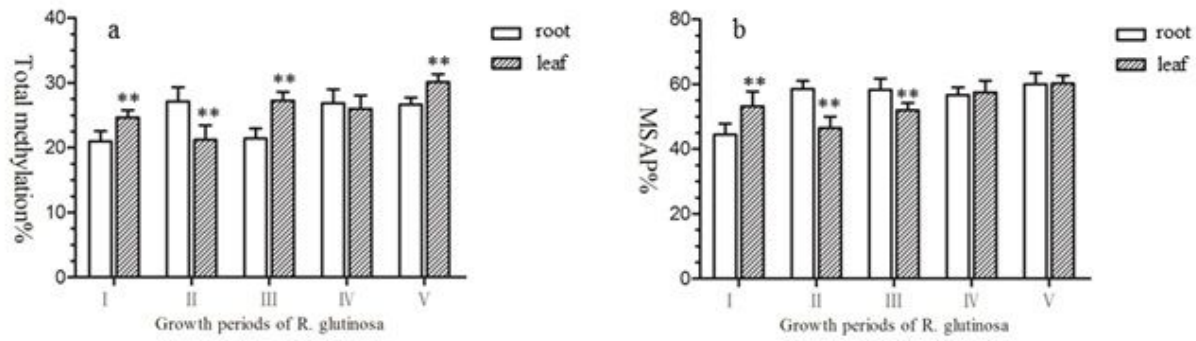


**Figure 4**

The genomic DNA methylation levels of *R. glutinosa* Total methylation ratio(%)= $\frac{\text{III}}{\text{I} + \text{II} + \text{III}} \times 100\%$ , MSAP(%)= $\frac{\text{II} + \text{III}}{\text{I} + \text{II} + \text{III}} \times 100\%$  statistical significance was determined by a two-sided t-test: \* P < 0.05, \*\* P < 0.01.

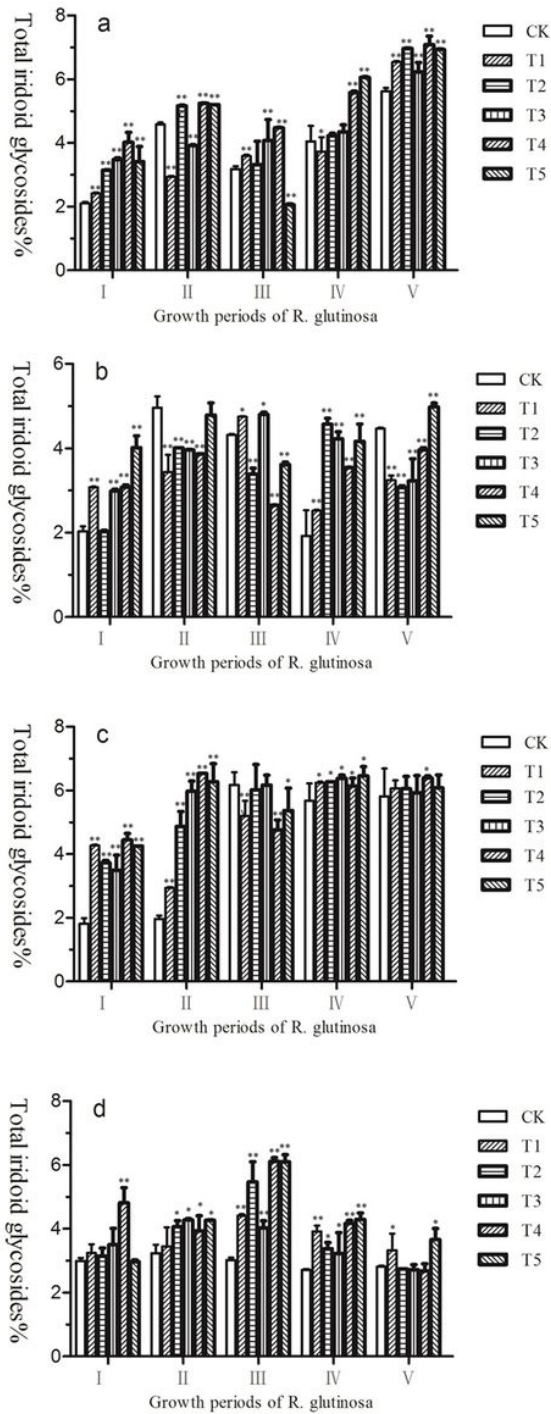


**Figure 5**

Effect of 5-azaC on total iridoid glycosides content of *R. glutinosa* a:85-5 root,b:85-5 leaf,c:Jinjiu root,d:Jinjiu leaf; CK, T1, T2, T3, T4 and T5 represent the 5-azaC treatment of 0 $\mu$ M, 15 $\mu$ M, 30 $\mu$ M, 50 $\mu$ M, 100 $\mu$ M and 250 $\mu$ M. statistical significance was determined by a two-sided t-test: \* P < 0.05, \*\* P < 0.01.

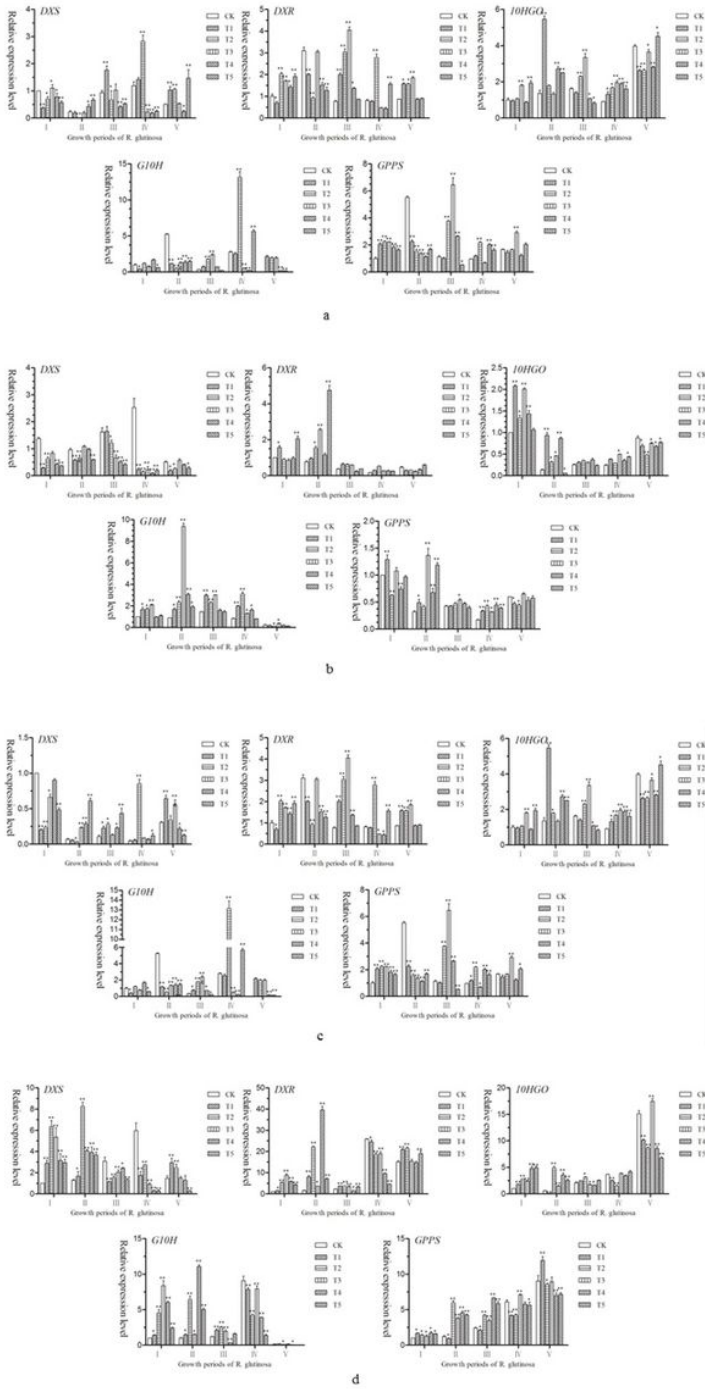


**Figure 6**

Effect of 5-azaC on expression of DXS,DXR,10HGO,G10G and GPPS a:85-5 root; b:Jinjiu root; c:85-5 leaf; d:Jinjiu leaf CK, T1, T2, T3, T4 and T5 represent the 5-azaC treatment of 0 $\mu$ M, 15 $\mu$ M, 30 $\mu$ M, 50 $\mu$ M, 100 $\mu$ M and 250 $\mu$ M. statistical significance was determined by a two-sided t-test: \*  $P < 0.05$ , \*\*  $P < 0.01$ .

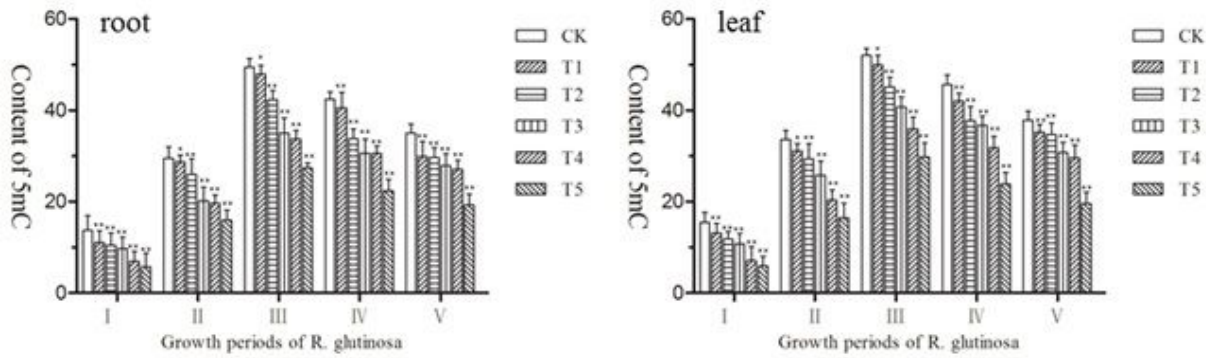


**Figure 7**

Effect of 5-azaC on 5mC content of *R. glutinosa* statistical significance was determined by a two-sided t-test: \*  $P < 0.05$ , \*\*  $P < 0.01$ .

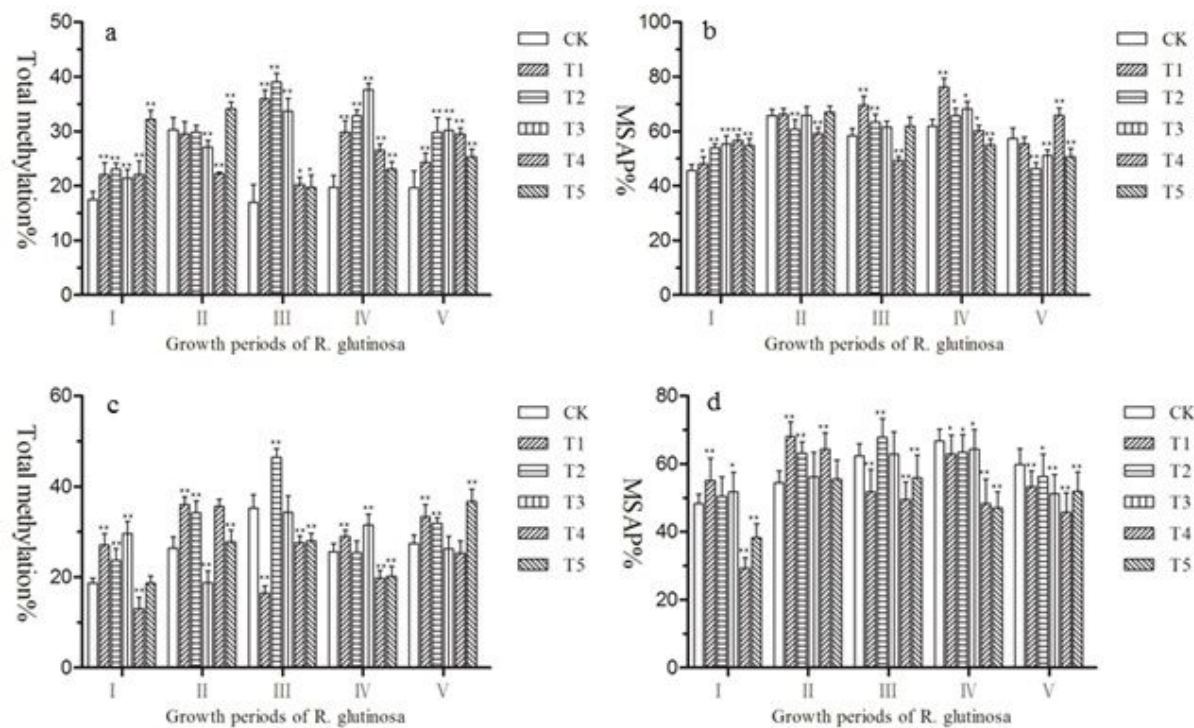


**Figure 8**

Effect of 5-azaC on genomic DNA methylation levels of *Rehmannia glutinosa* a: Total methylation% in root b: MSAP% in root c: Total methylation% in leaf d: MSAP% in leaf. Total methylation ratio(%) =  $\frac{III}{(I + II + III)} \times 100\%$ , MSAP(%) =  $\frac{(II + III)}{(I + II + III)} \times 100\%$  statistical significance was determined by a two-sided t-test: \*  $P < 0.05$ , \*\*  $P < 0.01$ .

## Supplementary Files

This is a list of supplementary files associated with this preprint. Click to download.

- [Supplementarymaterial.pdf](#)
- [Supplementarymaterial.pdf](#)